White Rose Research Online

eprints@whiterose.ac.uk
https://eprints.whiterose.ac.uk
Universities of Leeds, Sheffield and York

Deposited via The University of York.

White Rose Research Online URL for this paper:
https://eprints.whiterose.ac.uk/id/eprint/163615/

Version: Published Version

Article:
Lokotko, T., Leblond, S., Lee, J. et al. (2020) Shell structure of the neutron-rich isotopes Co 69,71,73. Physical Review C. 034314. ISSN: 2469-9993

https://doi.org/10.1103/PhysRevC.101.034314

Reuse
Items deposited in White Rose Research Online are protected by copyright, with all rights reserved unless indicated otherwise. They may be downloaded and/or printed for private study, or other acts as permitted by national copyright laws. The publisher or other rights holders may allow further reproduction and re-use of the full text version. This is indicated by the licence information on the White Rose Research Online record for the item.

Takedown
If you consider content in White Rose Research Online to be in breach of UK law, please notify us by emailing eprints@whiterose.ac.uk including the URL of the record and the reason for the withdrawal request.

Shell structure of the neutron-rich isotopes ^{69,71,73}Co

T. Lokotko,[1,*] S. Leblond,[1] J. Lee,[1,†] P. Doornenbal,[2] A. Obertelli,[3,2,‡] A. Poves,[4] F. Nowacki,[5] K. Ogata,[6,7] K. Yoshida,[8] G. Authelet,[3] H. Baba,[2] D. Calvet,[3] F. Château,[3] S. Chen,[1] A. Corsi,[3] A. Delbart,[3] J.-M. Gheller,[3] A. Gillibert,[3] T. Isobe,[2] V. Lapoux,[3] M. Matsushita,[10] S. Momiyama,[2,11] T. Motobayashi,[2] M. Niikura,[11] H. Otsu,[2] C. Péron,[3] A. Peyaud,[3] E. C. Pollacco,[3] J.-Y. Roussé,[3] H. Sakurai,[2,11] C. Santamaria,[3,2] Z. Y. Xu,[1] M. Sasano,[2] Y. Shiga,[2,12] S. Takeuchi,[2] R. Taniuchi,[2,11,§] T. Uesaka,[2] H. Wang,[2] V. Werner,[9] F. Browne,[13] L. X. Chung,[14] Zs. Dombradi,[15] S. Franchoo,[16] F. Giacoppo,[17] A. Gottardo,[16] K. Hadynska-Klek,[17] Z. Korkulu,[2,15] S. Koyama,[2,11] Y. Kubota,[2,10] M. Lettmann,[9] C. Louchart,[9] R. Lozeva,[5,18] K. Matsui,[2,11] T. Miyazaki,[2,11] S. Nishimura,[2] L. Olivier,[16] S. Ota,[10] Z. Patel,[19] E. Sahin,[17] C. Shand,[19] P.-A. Söderström,[2] I. Stefan,[16] D. Steppenbeck,[10] T. Sumikama,[20] D. Suzuki,[16] Zs. Vajta,[15] and J. Wu[2,21]

[1]*Department of Physics, The University of Hong Kong, Pokfulam, Hong Kong*
[2]*RIKEN Nishina Center, 2-1 Hirosawa, Wako, Saitama 351-0198, Japan*
[3]*CEA, Centre de Saclay, IRFU/Service de Physique Nucléaire, F-91191 Gif-sur-Yvette, France*
[4]*Departmento de Fisica Teorica and IFT-UAM/CSIC, Universidad Autónoma de Madrid, Madrid, Spain*
[5]*IPHC, IN2P3/CNRS, Université de Strasbourg, 67037 Strasbourg, France*
[6]*Research Center for Nuclear Physics (RCNP), Osaka University, Ibaraki 567-0047, Japan*
[7]*Department of Physics, Osaka City University, Osaka 558-8585, Japan*
[8]*Advanced Science Research Center, Japan Atomic Energy Agency, Tokai, Ibaraki 319-1195, Japan*
[9]*Institut für Kernphysik, Technische Universität Darmstadt, 64289 Darmstadt, Germany*
[10]*Center for Nuclear Study, University of Tokyo, RIKEN campus, Wako, Saitama 351-0198, Japan*
[11]*Department of Physics, University of Tokyo, 7-3-1 Hongo, Bunkyo-ku, Tokyo 113-0033, Japan*
[12]*Department of Physics, Rikkyo University, 3-34-1 Nishi-Ikebukuro, Toshima, Tokyo 172-8501, Japan*
[13]*School of Computing, Engineering and Mathematics, University of Brighton, Brighton BN2 4GJ, United Kingdom*
[14]*Institute for Nuclear Science & Technology, VINATOM, P.O. Box 5T-160, Nghia Do, Hanoi, Vietnam*
[15]*MTA Atomki, P.O. Box 51, Debrecen H-4001, Hungary*
[16]*Institut de Physique Nucléaire d'Orsay, IN2P3-CNRS, F-91406 Orsay Cedex, France*
[17]*Department of Physics, University of Oslo, N-0316 Oslo, Norway*
[18]*CSNSM, IN2P3/CNRS, Université Paris-Saclay, 91405 Orsay Campus, France*
[19]*Department of Physics, University of Surrey, Guildford GU2 7XH, United Kingdom*
[20]*Department of Physics, Tohoku University, Sendai 980-8578, Japan*
[21]*State Key Laboratory of Nuclear Physics and Technology, Peking University, Beijing 100871, People's Republic of China*

(Received 20 September 2019; revised manuscript received 21 February 2020; accepted 6 March 2020; published 30 March 2020)

The structures of the neutron-rich ^{69,71,73}Co isotopes were investigated via $(p, 2p)$ knockout reactions at the Radioactive Isotope Beam Factory, RIKEN. Isotopes of interest were studied using the DALI2 γ-ray detector array combined with the MINOS target and tracker system. Level schemes were reconstructed using the γ-γ coincidence technique, with tentative spin-parity assignments based on the measured inclusive and exclusive cross sections. Comparison with shell-model calculations using the Lenzi-Nowacki-Poves-Sieja LNPS and PFSDG-U interactions suggests coexistence of spherical and deformed shapes at low excitation energies in the ^{69,71,73}Co isotopes. The distorted-wave impulse approximation (DWIA) framework was used to calculate the single-particle cross sections. These values were compared with the experimental findings.

DOI: 10.1103/PhysRevC.101.034314

I. INTRODUCTION

Shape coexistence is one of the central topics in nuclear physics [1]. Investigations have shown that the shape of nuclei, described in terms of multipole moments (quadrupole, octupole, etc.), can vary greatly with a change of a few protons or neutrons [2,3]. Nuclei located in the valley of stability and close to proton and neutron magic numbers appear to be spherical, while isotopes in the mid-shell region are found to

*tlokotko@hku.hk
†jleehc@hku.hk
‡Present address: Institut für Kernphysik, Technische Universität Darmstadt, 64289 Darmstadt, Germany.
§Present address: Department of Physics, University of York, York YO10 5DD, United Kingdom.

 ©2020 American Physical Society

have deformed shapes [4–6]. Deformation in nuclei in general is caused by the quadrupole interaction [7,8]. Examination of shell evolution in regions far from stability is important for assessing nuclear models as new features arise, for instance new magic numbers [9–12] and rapid phase transitions [13]. For instance, ^{68}Ni has attracted much attention due to its neutron $N = 40$ harmonic oscillator magic number and proton magic number $Z = 28$ [14]. The observation of a high 2_1^+ excitation energy in ^{68}Ni has provided a clear signature for its magicity (spherical shape) in the ground state [15,16]. On the other hand, the 2_1^+ excitation energy of ^{66}Fe, which has only two protons removed, drops significantly, indicating a deformed shape [17,18]. The isotope ^{67}Co is located between ^{68}Ni and ^{66}Fe along the $N = 40$ isotonic chain, and, interestingly, experiment indicates that it exhibits shape coexistence [19–22].

Energy systematics of the odd-mass $^{55-67}$Co isotopes, presented in Ref. [19], show that the $9/2_1^-$ and $11/2_1^-$ excited states closely follow the corresponding 2_1^+ excitation energies in the neighboring Ni isotopes. Excited $9/2_1^-$ and $11/2_1^-$ states of ^{55}Co ($N = 28$) lie at approximately 3 MeV, very close to the 2_1^+ excitation energy of ^{56}Ni. With increasing neutron number, excited $9/2_1^-$ and $11/2_1^-$ states of ^{57}Co drop together with the 2_1^+ excitation energy of ^{58}Ni. This trend continues with slight variations along the even-odd Co isotopes, suggesting that these $9/2_1^-$ and $11/2_1^-$ levels can be approximated as $\pi f_{7/2}^{-1} \otimes 2_1^+$(Ni) configurations. For ^{67}Co, the heaviest isotope with tentatively assigned $9/2_1^-$ and $11/2_1^-$ levels, their rise in excitation energy is analogous to the rise in 2_1^+ excitation energy of ^{68}Ni and indicates spherical features.

Conversely, the observation of a low energy isomeric level at 492 keV [$T_{1/2} = 496(33)$ ms] with spin $1/2^-$ in the isotope ^{67}Co revealed the existence of a decay band with a different structure from a proton hole configuration, as this state was greatly decreased in energy compared to the excitations in ^{68}Ni [20]. This low-lying isomer configuration in ^{67}Co has been interpreted as a prolate proton-intruder state coupled to the ground state of the isotope ^{66}Fe [21]. The low-energy $1/2^-$–$3/2^-$ configuration is explained by strong proton-neutron correlations producing a deformed shape in ^{67}Co [20,21].

So far, among all neutron-rich Co nuclei only ^{67}Co has shown signs of shape coexistence. Together with indications of shape coexistence reported in ^{78}Ni [23], this raises the question regarding the shell evolution towards $N = 50$. The region beyond $N = 40$ is experimentally challenging, in particular β-decay studies of ^{71,73}Co offer only limited yield due to the very low production rates of ^{71,73}Fe secondary beams and large β-delayed neutron emission probabilities. In this work, the in-beam γ ray spectroscopy technique combined with the quasi-free $(p, 2p)$ reaction was chosen to establish level schemes of ^{69,71,73}Co. While γ-ray transitions have been measured for ^{69}Co, but not placed in the level scheme [24], hitherto no data were available on ^{71,73}Co.

II. EXPERIMENT

The experiment was carried out at the Radioactive Isotope Beam Factory, operated by the RIKEN Nishina Center and the Center for Nuclear Study, University of Tokyo, where radioactive isotopes of ^{70,72,74}Ni were produced by impinging a 345 MeV/u ^{238}U primary beam (with an average intensity of 12 p nA) onto a 3-mm-thick ^{9}Be target. Fragmentation products, which had an energy of ≈270 MeV/u, were separated and identified using the BigRIPS separator [25,26]. Two settings were applied to BigRIPS to produce the isotopes of interest. Particle identification on an event-by-event basis was performed via time of flight (ToF), magnetic rigidities ($B\rho$), and energy loss (ΔE) measurements. The ToF was measured between two plastic scintillators separated by 46.6 m, $B\rho$ was measured by trajectory reconstruction using position-sensitive parallel plate avalanche counters (PPAC) [27], and the energy loss was measured using a multiple sampling ionization chamber (MUSIC) [28]. Particle identification of the fragments of both BigRIPS settings is shown in Fig. 1.

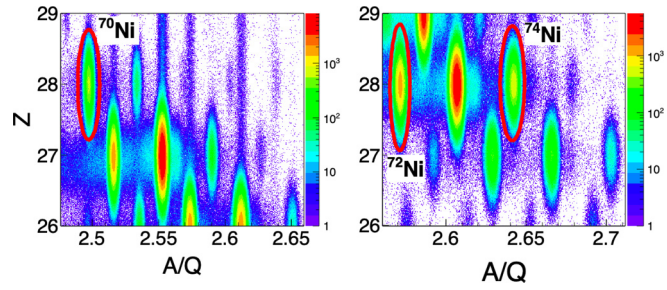

FIG. 1. Particle identification plots for radioactive ions passing BigRIPS for the first (left) and second settings (right).

Excited states of ^{69,71,73}Co were populated via $(p, 2p)$ reactions of ^{70,72,74}Ni secondary beams that had intensities of 90, 9, and 8 pps, respectively. The secondary beams were delivered to MINOS [29], a time projection chamber (TPC) surrounding a secondary target of 102(1) mm length filled with liquid hydrogen with an effective thickness of 735(8) mg/cm^2 [30]. Average center-of-target energies were 252, 241, and 234 MeV/u for the three secondary beams. The TPC was used to track protons from $(p, 2p)$ reactions in order to reconstruct the vertex of the reaction, thus improving resolution for Doppler corrections. The reaction vertex was reconstructed with a 95% efficiency for at least one proton tracked from the $(p, 2p)$ channel and with 5 mm resolution (FWHM) along the beam axis [31]. Reaction products exiting MINOS were identified with the ZeroDegree spectrometer [26] by the ToF-$B\rho$-ΔE technique. The particle identification of the reaction products is shown in Fig. 2.

The DALI2 NaI(Tl) detector array [32] measured prompt γ rays emitted following the reactions. DALI2 consisted of 186 NaI(Tl) crystals, covering angles from 12° to 96° in the laboratory frame (between target center and detector center) along the beam axis. Energy calibrations of the detectors were made using stationary ^{88}Y, ^{137}Cs, and ^{60}Co γ-ray sources. The energy resolution of the array was measured to be 9% (6%) (FWHM) for 662 keV (1333 keV) γ rays. Doppler corrections, using the reconstructed vertex position in MINOS, were made to obtain the excitation energies in the center-of-mass frame. An add-back procedure, with a maximum distance between two γ rays of 15 cm, was performed to improve

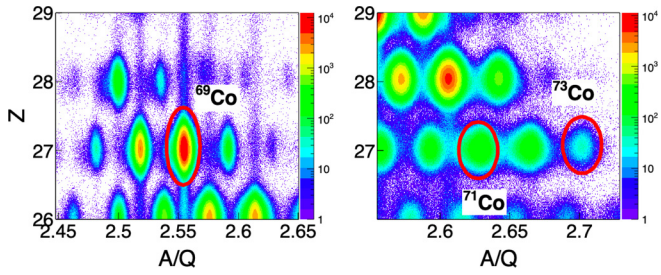

FIG. 2. Particle identification plots for radioactive ions arriving at ZeroDegree for the first (left) and second settings (right).

the peak-to-background ratio and photo-peak efficiency. The detection threshold was set to approximately 170 keV. From GEANT4 simulations [33], a full-energy photo-peak efficiency of 32% (20%) for 0.5 MeV (1 MeV) γ rays emitted at $\beta = 0.6$ was obtained prior to applying add-back procedures.

III. RESULTS

Transition energies for ^{69,71,73}Co measured in this work are listed in Table I together with energy uncertainties and relative γ ray intensities corrected for detection efficiency. Spin-parities of the excited states could not be determined by means of momentum distribution and angular correlations of γ rays due to resolution as the most limiting factor. Experimental data were fitted with generated detector response functions via GEANT4 simulations together with two exponential functions for the background. Intrinsic resolutions of individual DALI2 crystals with the 5 mm FWHM resolution in the vertex reconstruction were taken into account for the simulations. The energy calibration uncertainty (5 keV), statistical uncertainty, and systematic uncertainty were added in quadrature to deduce the final transition energy uncertainties. Lifetime estimates of low energy transitions in ^{69}Co were obtained from the minimization of χ^2 distributions as a function of transition energy and lifetime. The χ^2 values were obtained from the fitting of the experimental spectrum with simulated response functions in steps of 25 ps and 5 keV.

TABLE I. Summary of γ-ray transitions for ^{69,71,73}Co nuclei measured in the current experiment. Relative intensities for ^{69}Co were measured for $M_\gamma \leqslant 3$; those for ^{71,73}Co were measured for full gamma multiplicity M_γ.

Isotope	E_γ (keV)	τ (ps)	I_γ (%)	γ-γ (keV)	Literature
	240(11)	144(40)	48(6)		250 [24]
	287(11)	271(100)	31(6)		291 [24]
	427(11)	78(60)	29(6)		446 [24]
	488(11)		25(6)	1102	
^{69}Co	662(20)		15(6)		648, 663
					680 [24]
	1102(25)		54(8)	488	1105 [24]
	1285(8)		22(8)		
	1591(8)		100(8)		
	246(16)		100(34)		
^{71}Co	892(20)		93(54)	925	
	925(27)		88(56)		
	234(11)		20(10)		
	403(15)		20(16)		
^{73}Co	752(33)		100(24)	1044, 403	
	1044(37)		48(24)	752	
	1790(20)		82(30)		

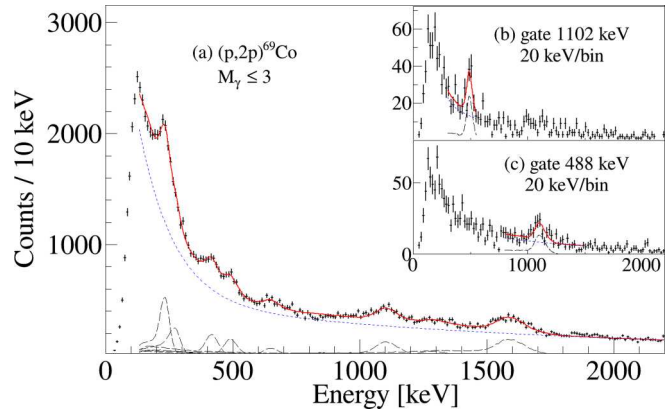

FIG. 3. (a) Doppler-corrected γ-ray spectrum for ^{69}Co populated via the ^{70}Ni$(p, 2p)^{69}$Co reaction. γ-γ coincidence spectra for the $(p, 2p)$ reaction are shown in the insets with a gate on the 1102-keV transition (b) and a gate on the 488-keV transition (c). The analysis was made for γ-ray multiplicity $M_\gamma = 2$ for (b) and $M_\gamma \leqslant 3$ for (c). Individual response functions for each transition are shown as long-dashed black curves, background as short-dashed red curves, and data fits as solid red curves.

Figure 3 presents Doppler-corrected spectra obtained from the ^{70}Ni$(p, 2p)^{69}$Co reaction. Two γ-γ coincidence spectra for the reaction are shown in the insets. For this isotope, transitions were observed at 240(11), 287(11), 427(11), 488(11), 662(20), 1102(25), 1285(8), and 1591(8) keV, of which the last one was the strongest [$I_{1591} = 100(8)\%$]. For the low energy transitions of 240(11), 287(11), and 427(11) keV, lifetimes were obtained to be 144(40), 271(100), and 78(60) ps respectively. Subsequent γ-γ analysis revealed coincidences between the 1102- and 488-keV transitions. As the sum of these two energies matches well with the 1591-keV transition, they are believed to originate from the same level. Intensity arguments put the 1102-keV transition [$I_{1102} = 54(8)\%$ with respect to the highest intensity γ] below the 488-keV transition [$I_{488} = 25(6)\%$]. Relative intensities of other transitions were measured to be the following: $I_{240} = 48(6)\%$, $I_{287} = 31(6)\%$, $I_{427} = 29(6)\%$, $I_{662} = 15(6)\%$, $I_{1285} = 22(8)\%$.

The Doppler-corrected γ-ray energy spectra in coincidence with the ^{72}Ni$(p, 2p)^{71}$Co reaction are presented in Fig. 4. Spectra were fitted in the same way as for ^{69}Co. Transition energies were observed at 246(16), 892(20), and 925(27) keV, with relative intensities of $I_{246} = 100(34)\%$, $I_{892} = 93(54)\%$, and $I_{925} = 88(56)\%$ with respect to the highest intensity γ. The latter two transitions were obtained from the self-coincidence of the 800–1050 keV region, which suggests the existence of two coincident γ-ray transitions merging into one structure in the spectrum. No γ-ray transitions were observed in coincidence with the 246-keV transition.

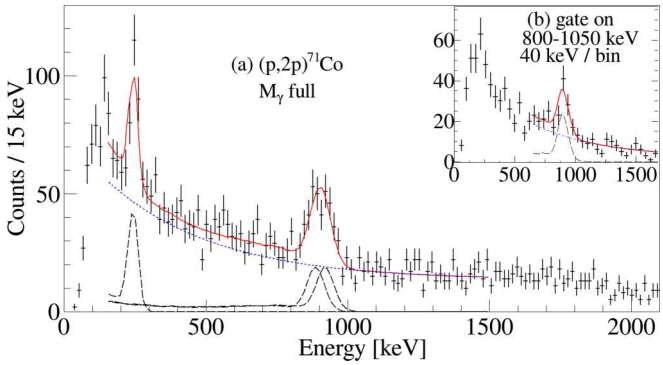

FIG. 4. (a) Doppler-corrected γ-ray spectrum for ^{71}Co populated via the $(p, 2p)$ reaction. Inset (b) shows the γ-γ coincidence spectrum with a gate on the 800–1050 keV region and considering all M_γ (background is not subtracted). Individual response functions for each transition are shown as long-dashed black curves, background as short-dashed red curves, and data fits as solid red curves.

The Doppler-corrected γ-ray spectrum following the ^{74}Ni$(p, 2p)$ ^{73}Co reaction is shown in Fig. 5. Transition energies were observed at 234(11), 403(15), 752(33), 1044(37), and 1790(20) keV. The measured relative intensities were $I_{234} = 20(10)\%$, $I_{403} = 20(16)\%$, $I_{752} = 100(24)\%$, $I_{1044} = 48(24)\%$, and $I_{1790} = 82(30)\%$ with respect to the highest intensity γ. The γ-γ coincidence analysis revealed that the 752-keV transition is in coincidence with the 1044-keV transition. Furthermore, the sum of the 752 and 1044-keV transitions corresponds, within error bars, to the 1790-keV transition. Therefore, it is assumed that they belong to the same decay branch, with intensity arguments putting the 752-keV transition of the cascade below the 1044-keV transition. Also the 752-keV transition was found to be in coincidence with the 403-keV transition. Possibly due to low statistics and low peak-to-background ratio, the 234-keV transition

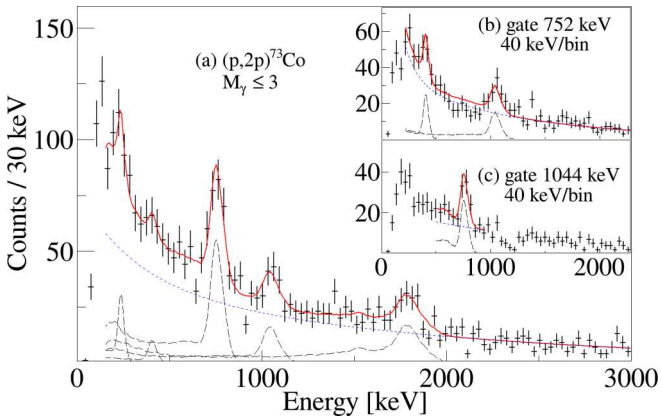

FIG. 5. (a) Doppler-corrected γ-ray spectrum for ^{73}Co populated via the $(p, 2p)$ reaction. γ-γ coincidence spectra are shown as insets without background subtraction and all M_γ, a gate on 752-keV (b), and a gate on 1044-keV (c). Individual response functions for each transition are shown as long-dashed black curves, background as short-dashed red curves, and data fits as solid red curves.

TABLE II. Inclusive and exclusive cross sections of the $(p, 2p)$ reaction channel for ^{69,71,73}Co nuclei. Exclusive cross sections are presented together with proposed values for J^π. The single-particle cross sections (σ_{sp}) were calculated from the DWIA framework. See text for details.

Isotope	J^π	E_{ex} (keV)	σ_{ex} (mb)	σ_{sp} (mb)	σ_{ex}/σ_{sp}
^{69}Co	$(7/2^-_1)$	0	<9.6(6)	1.70	<5.6(9)
	$(9/2^-_1)$	1102_{sph}	<0.7(1)		
	$(7/2^-_2)$	1591_{sph}	2.8(2)	1.66	1.7(3)
	inclusive		13.1(6)		
^{71}Co	$(7/2^-_1)$	0	<6.6(17)	1.54	<4.3(13)
	$(9/2^-_1)$	892_{sph}	0.0(10)		
	$(7/2^-_2)$	1817_{sph}	1.6(8)	1.44	1.1(6)
		246_{def}	1.5(6)		
	inclusive		9.7(6)		
^{73}Co	$(7/2^-_1)$	0	<6.0(14)	1.40	<4.3(12)
	$(9/2^-_1)$	752_{sph}	0.0(10)		
	$(7/2^-_2)$	1790_{sph}	1.5(6)	1.36	1.1(5)
	inclusive		8.0(10)		

was not clearly observed in γ-γ coincidence. Proposed level schemes for ^{69,71,73}Co nuclei are presented in Fig. 6.

Inclusive and exclusive cross sections of the $(p, 2p)$ reaction channels for ^{69,71,73}Co are presented in Table II. Transmission coefficients of ZeroDegree and reaction losses in the secondary target were taken into account in the extraction of the cross sections. Cross sections to the ground state, $\sigma_{g.s.}$, were estimated by subtracting the sum of exclusive cross sections σ_{ex} to excited states from the inclusive cross section σ_{inc}. Due to pandemonium effects and the unplaced transitions they represent upper limits. The ratio $\sigma_{g.s.}/\sigma_{inc}$ was then estimated to be less or equal to 73(10)%, 68(18)%, and 73(20)% for ^{69,71,73}Co nuclei, respectively. Quoted uncertainties of exclusive cross sections also include statistical uncertainties arising from the of γ-ray intensities.

IV. DISCUSSION

Level schemes for ^{69,71,73}Co nuclei were reconstructed based on γ-ray transitions showing clear coincidences with each other. They are presented in Fig. 6. The γ-ray coincidence analysis for ^{69}Co has shown clear existence of one independent decay path, consisting of the 1102- and 1591-keV levels. Energies of the γ rays for ^{69}Co, measured in the current experiment, are in good agreement with data from literature [24]. Transition energies of 1102(25) and 662(20) keV are in good agreement with the 1105-keV transition and the 648, 663, 680-keV triplet observed following β-decay [24]. Despite similarity between the 1591(8)-keV transition and the reported 1582-keV transition [24], it is suggested that the two transitions originate from different energy levels. This is supported by the absence of the 488(11)-keV transition in the previous experiment. The observed γ rays with energies of 240(11) and 287(11) keV, which were not placed in the level scheme, agree well with the 250- and 291-keV transitions

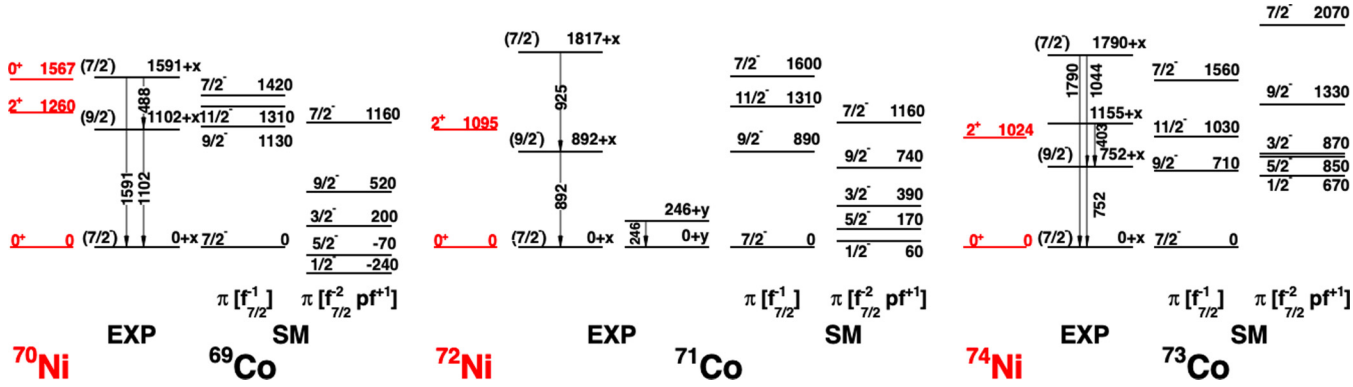

FIG. 6. Proposed level schemes and tentative spin-parity assignments for ^{69,71,73}Co according to shell-model calculations using the LNPS and PFSDG-U interactions. The relative position of spherical and deformed states was not measured during the experiment. The relative position of decay bands is defined with respect to x and y shifts, which can take on different values for each level scheme. Values of 0^+ and 2^+ Ni states are taken from Refs. [34,47]. See text for details.

observed in β decay [24]. The observed 427(11)-keV transition may correspond to the 446-keV transition from Ref. [24].

Shell model calculations for ^{69,71}Co were carried out in the $pf_{5/2}g_{9/2}d_{5/2}$ valence space [35] using the LNPS interaction [35] and for ^{73}Co in the pf-sdg valence space using the PFSDG-U interaction [36]. Calculated level schemes for ^{69,71,73}Co are shown in Fig. 6 next to their experimental counterparts. Two structures are predicted for all three Co isotopes: A "spherical" band, which corresponds to $\pi f_{7/2}^{-1}$ proton hole states, and a low-lying "deformed" $K = 1/2^-$ band that corresponds to $\pi f_{7/2}^{-2} pf^{+1}$ states. Deformation parameters of the $K = 1/2^-$ band for each isotope can be found in Table III. The energy levels of ^{69}Co measured in the current experiment at 1102 and 1591 keV are in good agreement with the predicted $9/2^-$ and $7/2^-$ spherical states at 1130 and 1420 keV, which can be interpreted as members of the $\pi f_{7/2}^{-1} \otimes 2_1^+$ (^{70}Ni) multiplet in a weak coupling scheme.

In addition, ^{69}Co may feature the existence of a low-lying deformed band. These states may be populated in the $(p, 2p)$ reactions by removal of a proton from the $p_{3/2}$ or $f_{5/2}$ orbital when two $f_{7/2}$ protons are elevated above the $Z = 28$ shell to the $0^+_{g.s.}$ in the corresponding nickel isotope. For ^{62,64}Ni it was estimated that the $p_{3/2}$ orbital is filled up to 12% [37,38], and a similar shell structure is expected in heavier Ni nuclei. "Deformed" states are interpreted in the shell model as members of a strongly coupled $K = 1/2^-$ band, which has a $(1p\text{-}2h + 2p\text{-}3h)$ structure across $Z = 28$ for protons and $(4p\text{-}4h)$ across $N = 40$ for neutrons. The relative position of the $1/2^-_{\rm def}$ and $7/2^-_{\rm sph}$ bands can be identified by measuring an $M3$, $1/2^- \rightarrow 7/2^-$ transition, as already discussed in Ref. [24] for ^{69}Co. It was impossible to measure transitions with long lifetimes with the current experimental setup. We further note that the existence of a low-lying, prolate deformed 0^+_2 1567-keV level was reported in Ref. [34] and well described theoretically in Ref. [16]. A proton hole $7/2^-$ state coupled to this deformed 0^+_2 state would produce a deformed, excited state in ^{69}Co at similar excitation energy. It is stressed, however, that the present knockout experiment was only sensitive to the overlaps between the states in the Co isotopes and the ground state of the corresponding Ni isotopes.

Also the level schemes of ^{71,73}Co may have low-lying bands, as evinced by the low-energy γ-ray transitions, in addition to the spherical states. Indeed, such bands are predicted with the the LNPS and PFSDG-U interactions, as shown in Fig. 6. In ^{71}Co, the observed excited state at 1818 keV likely corresponds to the predicted $7/2^-$ level at 1600 keV, while the experimental level at 892 keV corresponds to the $9/2^-$ level, in agreement with expected decay patterns. Since the 246-keV transition was not found in coincidence with the transitions from spherical states, it is suggested that this transition belongs to the deformed band. The 246-keV transition likely corresponds to either the predicted $5/2^- \rightarrow 1/2^-$ transition or the $3/2^- \rightarrow 5/2^-$ transition. The isotope ^{73}Co manifests a similar level scheme. The experimental level at 1790 keV is well matched by the predicted $7/2^-$ level at 1560 keV. Likewise, the experimental level at 752 keV corresponds to the predicted $9/2^-$ counterpart at 710 keV. Analogously, the experimental transition at 234 keV may correspond to a transition between the predicted deformed $3/2^-$ or $5/2^-$ levels at 870 and 850 keV decaying into the $1/2^-$ level at 670 keV. As for ^{69}Co, no relative position of $1/2^-_{\rm def}$ and $7/2^-_{\rm sph}$ states in ^{71,73}Co was determined with the current experimental setup.

Inclusive and exclusive cross sections presented in Table II provide more insights on the shell structure of ^{69,71,73}Co isotopes. Cross sections to the ground state were evaluated to be less than or equal to 70% with respect to the inclusive cross sections for ^{69,71,73}Co isotopes. The tentative spin-parity assignments of excited states of ^{69,71,73}Co isotopes can be

TABLE III. Properties of the deformed $K = 1/2^-$ bands in ^{69,71,73}Co obtained from shell-model calculations. The LNPS interaction was used for ^{69,71}Co and the PFSDG-U interaction for ^{73}Co.

	^{69}Co	^{71}Co	^{73}Co
Quadrupole moment Q_0 (e fm^2)	300	290	320
Deformation parameter (β)	0.3	0.3	0.3
$B(E2, 5/2^- \rightarrow 1/2^-)$ (e^2fm^4)	500	440	420
$E(1/2^-)_{\rm def} - E(7/2^-)_{\rm sph}$ (keV)	−240	+60	+670

corroborated by these cross sections. In a single-particle model, the knockout of an $f_{7/2}$ proton from Ni isotopes by the $(p, 2p)$ reaction simply results in the $7/2^-$ ground state of the respective Co isotope. This argument is supported by the large spectroscopic factors to the $7/2^-$ ground states extracted for ^{61,63}Co nuclei [38–41]. These studies also found spectroscopic factors of $C^2S \approx 0.6$ for the first excited $7/2^-$ state.

Theoretical single-particle cross sections, $\sigma_{\rm sp}$, presented in Table II, were calculated in the distorted wave impulse approximation (DWIA) framework [42] and averaged along the target length. The Bohr-Mottelson single-particle potential [43] was used to obtain the single-particle wave function and the nuclear density. The depth of the potential was adjusted to reproduce the single-particle energy. The microscopic folding model [44] with the Melbourne g-matrix interaction [45] and the calculated nuclear density was used to construct the optical potentials for the distorted waves in the initial and final channels. The spin-orbit part of distorting potentials was disregarded. The pp interaction was adopted from the Franey-Love effective interaction [46]. This approach is estimated to provide theoretical single-particle cross sections with a systematic uncertainty of 15% [42]. It resulted in ground state ratios $(\sigma^{ex}_{g.s}/\sigma_{\rm sp})$ of 5.6(9), 4.3(13), and 4.3(12) for ^{69,71,73}Co isotopes, respectively. These values are similar to the ground state spectroscopic factors obtained for ^{61,63}Co nuclei [38–41], but it must be stressed that due to unobserved feeding and the unplaced transitions the obtained values in the present work are only upper limits. Similarly, large values of $\sigma_{\rm ex}$ suggest an assignment of the second-excited state of the spherical band in the ^{69,71,73}Co nuclei to be $J^\pi = 7/2^-$. Moreover, shell-model calculations and decay patterns then suggest the first-excited state of the spherical band in ^{69,71,73}Co to have a spin-parity of $J^\pi = 9/2^-$. This state cannot be directly populated by the $(p, 2p)$ reaction, but through feeding from higher-lying excited states. Indeed, low cross sections were observed for the tentatively assigned $9/2^-$ states.

Finally, it is interesting to compare the energy systematics between the $9/2^-_1$ states relative to the $7/2^-_1$ states—for most isotopes it is the ground state—in the ^{69,71,73}Co isotopic chain and the corresponding 2^+_1 excitation energies for the Ni isotopes. The comparison displayed in Fig. 6 reveals a clear correlation between the $9/2^-_1$ states and respective 2^+_1 excitations in the Ni isotopes. This tendency suggests that the $9/2^-_1$ states of Co isotopes are part of the $\pi f^{-1}_{7/2} \otimes 2^+_1$(Ni) multiplet. The significant drop of the $9/2^-_1$ energies in ^{69,71,73}Co isotopes, compared to $9/2^-_1$ of ^{67}Co reported in [19–22], may be understood as an increase of the paring correlations between protons and neutrons. Shell model calculations presented in Table III also support the changes in shell structure of the Co isotopes, as the intrinsic (mass) quadrupole moment Q_0 increases by $\approx$120 $e\,$fm^2 from $Q_0 = 180\ e\,$fm^2 (calculated in Ref. [19]) for ^{67}Co to $Q_0 \approx 300\ e\,$fm^2 for ^{69,71,73}Co.

V. SUMMARY AND CONCLUSIONS

In the present work, excited states in neutron-rich odd-even ^{69,71,73}Co nuclei have been populated via quasi-free $(p, 2p)$ knockout reactions. BigRIPS and ZeroDegree spectrometers were used together with the DALI2 array and the MINOS hydrogen target and TPC to extract their excitation energies. Level schemes were reconstructed via γ-γ analysis for the first time. Large-scale shell-model calculations using LNPS and PFSDG-U effective interactions were confronted with our experimental findings. Spin-parity of reconstructed levels were proposed based on the measured inclusive and exclusive cross sections. The single-particle cross sections, calculated in DWIA, were used to evaluate the ratio between $\sigma_{\rm ex}$ and $\sigma_{\rm sp}$. Tentatively assigned $9/2^-_1$ states of ^{69,71,73}Co isotopes follow the trend of the 2^+_1 level energies of the nickel isotopes. Taking into account the systematic behavior and the good agreement with shell-model calculations, the excited $7/2^-$ and $9/2^-$ states can be interpreted as $\pi f^{-1}_{7/2} \otimes 2^+$(Ni) configurations.

ACKNOWLEDGMENTS

The authors are thankful to the RIBF and RIKEN accelerator teams for stable operation of the uranium primary beam during the experiment and the production of the secondary beams. We acknowledge the support by the University of Hong Kong within RGC Early Career Scheme (ECS) (Contract No. 27303915). The development of MINOS and the core MINOS team have been supported by the European Research Council through the ERC Grant No. MINOS-258567. A.O. has been supported by the JSPS long-term fellowship L-13520 at the RIKEN Nishina Center. C.S. has been supported by the IPA program at the RIKEN Nishina Center. A.P. has been supported by the Ministerio de Ciencia, Innovacion y Universidades (Spain), Severo Ochoa Prog. SEV-2016-0597 and Grant No. PGC-2018-94583. L.X.C would like to thank MOST for its support through the Physics Development Program Grant No. ĐTĐLCN.25/18. R.T. has been supported by the JSPS Grant-in-Aid for JSPS Research Fellows JP14J08718. K.O. acknowledges the support by Grant-in-Aid for Scientific Research JP16K05352.

[1] K. Heyde and J. L. Wood, Rev. Mod. Phys. **83**, 1467 (2011).
[2] F. Iachello and I. Talmi, Rev. Mod. Phys. **59**, 339 (1987).
[3] E. Caurier, G. Martinez-Pinedo, F. Nowack, A. Poves, and A. P. Zuker, Rev. Mod. Phys. **77**, 427 (2005).
[4] R. F. Casten, *Nuclear Structure from a Simple Perspective* (Oxford University Press, Oxford, 2005).
[5] P. Vingerhoets *et al.*, Phys. Rev. C **82**, 064311 (2010).
[6] H. Sagawa, X. R. Zhou, and X. Z. Zhang, Phys. Rev. C **72**, 054311 (2005).
[7] A. Bohr and B. Mottelson, *Nuclear Structure* (Benjamin, New York, 1975), Vol. II.
[8] I. Hamamoto, Phys. Rev. C **85**, 064329 (2012).
[9] M. Rejmund *et al.*, Phys. Rev. C **76**, 021304(R) (2007).
[10] A. Ozawa, T. Kobayashi, T. Suzuki, K. Yoshida, and I. Tanihata, Phys. Rev. Lett. **84**, 5493 (2000).

[11] R. Kanungo *et al.*, Phys. Rev. Lett **88**, 142502 (2002).
[12] B. A. Brown and W. A. Richter, Phys. Rev. C **72**, 057301 (2005).
[13] T. Togashi, Y. Tsunoda, T. Otsuka, and N. Shimizu, Phys. Rev. Lett. **117**, 172502 (2016).
[14] R. Broda *et al.*, Phys. Rev. Lett. **74**, 868 (1995).
[15] S. Suchyta, S. N. Liddick, Y. Tsunoda, T. Otsuka, M. B. Bennett, A. Chemey, M. Honma, N. Larson, C. J. Prokop, S. J. Quinn, N. Shimizu, A. Simon, A. Spyrou, V. Tripathi, Y. Utsuno, and J. M. VonMoss, Phys. Rev. C **89**, 021301(R) (2014).
[16] Y. Tsunoda, T. Otsuka, N. Shimizu, M. Honma, and Y. Utsuno, Phys. Rev. C **89**, 031301(R) (2014).
[17] A. Gade, R. V. F. Janssens, T. Baugher, D. Bazin, B. A. Brown, M. P. Carpenter, C. J. Chiara, A. N. Deacon, S. J. Freeman, G. F. Grinyer, C. R. Hoffman, B. P. Kay, F. G. Kondev, T. Lauritsen, S. McDaniel, K. Meierbachtol, A. Ratkiewicz, S. R. Stroberg, K. A. Walsh, D. Weisshaar, R. Winkler, and S. Zhu, Phys. Rev. C **81**, 051304(R) (2010).
[18] J. Kotila and S. M. Lenzi, Phys. Rev. C **89**, 064304 (2014).
[19] F. Recchia *et al.*, Phys. Rev. C **85**, 064305 (2012).
[20] D. Pauwels *et al.*, Phys. Rev. C **78**, 041307(R) (2008).
[21] D. Pauwels *et al.*, Phys. Rev. C **79**, 044309 (2009).
[22] W. Walters *et al.*, in *Nuclear Structure and Dynamics '15*, 14–19 June 2015, Portoroš, Slovenia, edited by M. Lipoglavšek, M. Milin, T. Nikšić, S. Szilner, and D. Vretenar, AIP Conf. Proc. No. 1681 (AIP, New York, 2015), p. 030007.
[23] R. Taniuchi *et al.*, Nature (London) **569**, 53 (2019).
[24] S. N. Liddick *et al.*, Phys. Rev. C **92**, 024319 (2015).
[25] N. Fukuda *et al.*, Nucl. Instrum. Methods Phys. Res. B **317**, 323 (2013).
[26] T. Kubo *et al.*, Prog. Theor. Exp. Phys. **2012**, 03C003 (2012).
[27] H. Kumagai *et al.*, Nucl. Instrum. Methods Phys. Res. A **470**, 562 (2001).
[28] K. Kimura *et al.*, Nucl. Instrum. Methods Phys. Res. A **538**, 608 (2005).
[29] A. Obertelli, A. Delbart, S. Anvar *et al.*, Eur. Phys. J. A **50**, 8 (2014).
[30] C. Santamaria *et al.*, Phys. Rev. Lett. **115**, 192501 (2015).
[31] C. Santamaria *et al.*, Tracking with the MINOS Time Projection Chamber. Nuclear Inst. and Methods in Physics Research, A (2018).
[32] S. Takeuchi *et al.*, Nucl. Instrum. Methods Phys. Res. A **763**, 596 (2014).
[33] S. Agostinelli *et al.*, Nucl. Instrum. Methods Phys. Res. A **506**, 250 (2003).
[34] C. J. Prokop *et al.*, Phys. Rev. C **92**, 061302(R) (2015).
[35] S. M. Lenzi, F. Nowacki, A. Poves, and K. Sieja, Phys. Rev. C **82**, 054301 (2010).
[36] F. Nowacki, A. Poves, E. Caurier, and B. Bounthong, Phys. Rev. Lett. **117**, 272501 (2016).
[37] A. G. Blair, Phys. Rev. **140**, B648 (1965).
[38] A. G. Blair and D. D. Armstrong, Phys. Rev. **151**, 930 (1966).
[39] F. R. Hudson and R. N. Glover, Nucl. Phys. A **160**, 482 (1971).
[40] Ole Hansen *et al.*, Nucl. Phys. A **313**, 95 (1979).
[41] M. Seeger *et al.*, Nucl. Phys. A **533**, 1 (1991).
[42] T. Wakasa, K. Ogata, and T. Noro, Prog. Part. Nucl. Phys. **96**, 32 (2017).
[43] A. Bohr and B. Mottelson, *Nuclear Structure* (Benjamin, New York, 1969), Vol. I.
[44] M. Toyokawa, K. Minomo, and M. Yahiro, Phys. Rev. C **88**, 054602 (2013).
[45] K. Amos, P. Dortmans, H. von Geramb, S. Karataglidis, and J. Raynal, in *Advances in Nuclear Physics*, edited by J. W. Negele and E. Vogt, Vol. 25 (Springer, Boston, MA), pp. 276–536.
[46] M. A. Franey and W. G. Love, Phys. Rev. C **31**, 488 (1985).
[47] http://www.nndc.bnl.gov/.